Triptycene Walled Glycoluril Trimer: Synthesis and Recognition Properties

Journal:	*New Journal of Chemistry*
Manuscript ID	NJ-ART-10-2019-005336.R1
Article Type:	Paper
Date Submitted by the Author:	25-Nov-2019
Complete List of Authors:	Ndendjio, Sandra; University of Maryland at College Park, Chemistry and Biochemistry Liu, Wenjin; Beijing Institute of Technology, Chemistry Yvanez, Nicolas; Ecole Nationale Superieure de Chimie de Paris Meng, Zihui; Beijing Institute of Technology, Chemistry Zavalij, Peter; University of Maryland at College Park Department of Chemistry and Biochemistry, Isaacs, Lyle; University of Maryland at College Park, Chemistry and Biochemistry

Journal Name

FULL PAPER

Triptycene Walled Glycoluril Trimer: Synthesis and Recognition Properties

Received 00th January 20xx,
Accepted 00th January 20xx

DOI: 10.1039/x0xx00000x

www.rsc.org/

Sandra Zebaze Ndendjio,[a] Wenjin Liu,[a,b] Nicolas Yvanez,[a,c] Zihui Meng,[b,*] Peter Y. Zavalij,[a] and Lyle Isaacs[a,*]

We report the synthesis of a new acyclic CB[n]-type host (1) that features a central glycoluril trimer capped by triptycene sidewalls. Host 1 has good solubility in water (≈ 3 mM) and does not undergo strong self-association (K_s = 480 M^{-1}). We probed the geometry of the complexes by analyzing the complexation induced changes in the ^{1}H NMR spectra and measured the complexation thermodynamics by isothermal titration calorimetry. The conformation of 1 and its packing in the solid state was revealed by single crystal x-ray diffraction measurements.

Introduction

The synthesis and molecular recognition properties of the cucurbit[n]uril (CB[n]) family of molecular container compounds has undergone rapid development since the turn of the millennium.[1] Figure 1 shows the molecular structure of CB[*n*] which are composed of *n* glycoluril units connected by *2n* methylene bridges that form a barrel shaped macrocycle with two electrostatically negative ureidyl carbonyl fringed portals and a central hydrophobic cavity. Accordingly, macrocyclic CB[n] bind tightly to hydrophobic (di)ammonium ions in water with binding constants typically in the $10^6 - 10^{12}$ M^{-1} range, even exceeding 10^{17} M^{-1} in special cases.[2] The very high affinity of CB[n]•guest complex has been traced, in part to the presence of intracavity waters that lack a full complement of H-bonds that are released upon complexation.[3] Accordingly, the K_a values for CB[n]•guest complexes have been featured prominently in a series of blinded challenges (SAMPL and Hydrophobe) that aim to improve computational approaches to free energy calculations in water.[4] CB[n]•guest complexes respond sensitively to appropriate stimuli (e.g. pH, chemical, electrochemical, photochemical)[5] allowing them to be used as a high fidelity switching element in complex systems. Accordingly, unfunctionalized macrocyclic CB[n] has found numerous uses including as a component of (bio)sensing ensembles,[6] for drug formulation, delivery and sequestration,[7] to create supramolecular organic frameworks,[8] and to perform supramolecular catalysis.[3c] With the development of functionalized CB[n], the range of application has been expanded to include CB[n] based targeted drug delivery and theranostics, materials for protein capture, supramolecular Velcro, and nanoparticle based optical assays.[9]

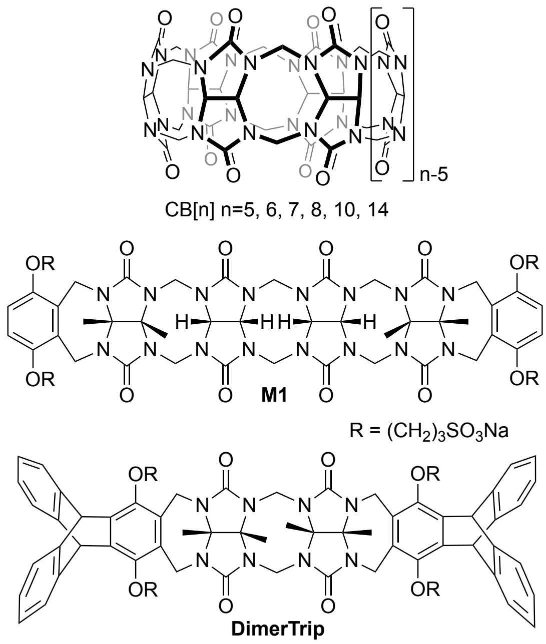

Figure 1 Structure of CB[n] (n = 5, 6, 7, 8, 10, 14), acyclic CB[n]-type receptor **M1**, and **DimerTrip.**

In recent years, we and others have been studying acyclic CB[n]-type receptors that feature a central glycoluril oligomer (e.g. dimer – tetramer) that is capped by aromatic sidewalls.[10a, 10b, 1d,

a. *Department of Chemistry and Biochemistry, University of Maryland, College Park, Maryland 20742, USA. E-mail: lisaacs@umd.edu.*
b. *School of Chemistry and Chemical Engineering, Beijing Institute of Technology, 5 South Zhongguancun Street, Beijing 100081, P. R. China*
c École Nationale Supérieure de Chimie de Paris, 11 rue Pierre et Marie Curie, F75231 Paris cedex 05, France
† Electronic Supplementary Information (ESI) available: Details of synthesis, NMR, and ITC experiments. See DOI: 10.1039/x0xx00000x

[10c, 10d] Figure 1 shows the structure of the prototypical acyclic CB[n] (**M1**) which features a central glycoluril tetramer, *o*-xylylene sidewalls, and sulfonate solubilizing groups. **M1** shows excellent biocompatibility according to a variety of *in vitro* and *in vivo* assays[11] and is therefore considered for real world applications. For example, **M1** and analogues have been used as solubilizing excipients for insoluble drugs,[12] for pH triggered delivery agents,[13] as *in vivo* sequestration agents for neuromuscular blockers and drugs of abuse,[14] and as components of sensing arrays.[15] Most recently, we have created chimeric receptors comprising glycoluril monomer, dimer, or tetramer units with triptycene sidewalls with the goal of increasing binding capacity and binding strength and observed interesting behavior like triggered decomposition of vesicles and the ability to wrap around macrocyclic guests.[16] In this paper we prepare acyclic CB[n]-type host **1** derived from glycoluril trimer, investigate its binding properties toward alkylammonium ions to elucidate its basic recognition properties and to serve as a blinded dataset for the SAMPL7 challenge,[17] and finally to assess its potential as as a sequestration agent toward drugs of abuse.

Results and Discussion

This results and discussion section is organized as follows. First, we present the design, synthesis, and characterization of host **1**. Next, we quantify the self-association propensity of **1** and perform qualitative ^{1}H NMR based host•guest complexation studies. Subsequently, we measure the complexation thermodynamic parameters by isothermal titration calorimetry (ITC) and discuss the observed structure-binding constant trends.

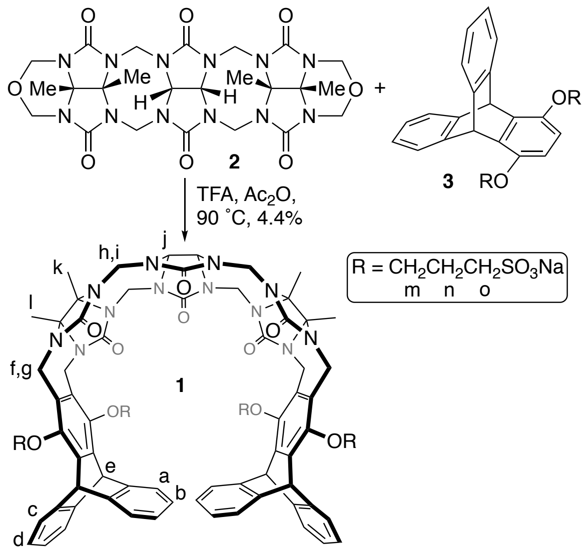

Figure 2 Synthesis of host **1**.

Design, Synthesis, and Characterization of Host 1. The synthesis of host **1** is based on our previously described building block approach[1d] involving the electrophilic aromatic substitution reactions between glycoluril bis(cyclic ethers) and activated aromatic rings. Accordingly, we reacted glycoluril trimer **2**[18] with triptycene derivative **3**[16c] under acidic conditions (TFA, Ac_2O) which delivered crude **1** after precipitation with EtOH. Purification of **1** was challenging and required a combination of washing with EtOH and acetone followed by recrystallization from mixtures of EtOH and H_2O to deliver **1** in 4.4% isolated yield. The chemical structure of **1** was fully elucidated by spectroscopic means and was further confirmed by single crystal x-ray diffraction studies (*vide infra*). The ^{1}H NMR spectrum of **1** in D_2O shows a single resonance for the glycoluril methine protons (H_j), two pairs of resonances for the diastereotopic methylene bridges ($H_{f,g}$ and $H_{h,i}$), two CH_3-groups (k and l), and two pairs of aromatic protons ($H_{a,b}$ and $H_{c,d}$). The number of resonances is fully consistent with the time-averaged C_{2v}-symmetry depicted in Figure 2. However, the resonance for H_b on the tip of the aromatic ring is upfield shifts and appears at 5.7 ppm which suggests that uncomplexed **1** assumes a self-folded conformation in water (*vide infra*) similar to previously prepared triptycene walled glycoluril tetramer.[16c] The ^{13}C NMR spectrum for **1** recorded in DMSO-d_6 displays 22 resonances which is also in agreement with time averaged C_{2v}-symmetry. Finally, the high resolution ESI-MS spectrum of **1** shows a doubly charged ion at *m/z* 829.20204 which is in accord with the calculated value ($C_{76}H_{75}N_{12}NaO_{22}S_4$, $[M + 1H - 3Na]^{2-}$, calculated 829.19495).

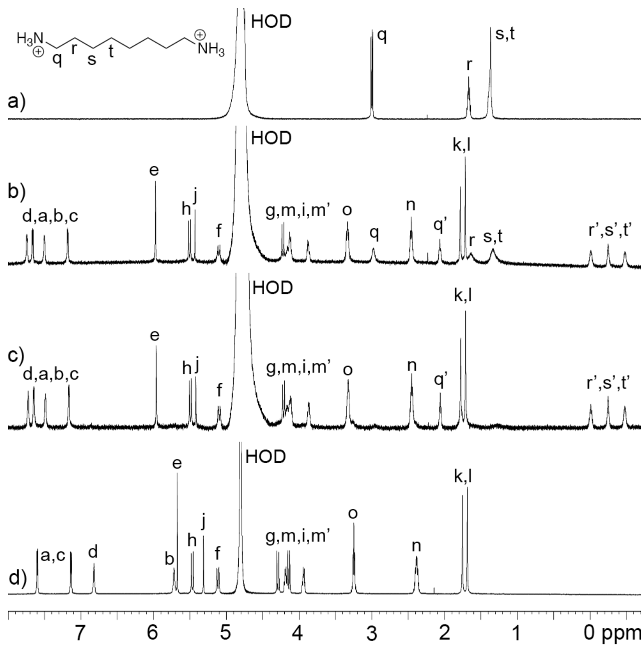

Figure 3 ^{1}H NMR spectra recorded (600 MHz, RT, 20 mM sodium phosphate buffered D_2O, pH 7.0) for: a) guest **8** (2 mM), b) a mixture of **1** (250 µM) and **8** (500 µM), c) a mixture of **1** (250 µM) and **8** (250 µM), and d) host **1** (250 µM).

Self-Association Properties of Host 1. Before proceeding to investigate the host•guest properties of **1** we perform dilution studies to quantify the extent of self-association of **1**.[19] Accordingly, we measured the ^{1}H NMR spectra of a series of solutions of **1** in D_2O from its solubility limit of 3 mM down to 0.05 mM (Figure S4). We observe small changes in chemical shift of many protons including H_b, $H_{k/l}$, and H_f. Figure 4 shows a plot of the concentration of **1** versus chemical shift of H_b that was fitted to a dimerization model in Scientist™ (Supporting

Please do not adjust margins

Information) which allowed us to extract the self-association constant (K_s = 480 ± 81 M^{-1}). The measurement of the thermodynamic parameters of complexation of **1** (*vide infra*) were measured by ITC at [**1**] = 100 μM where the host remains monomeric.

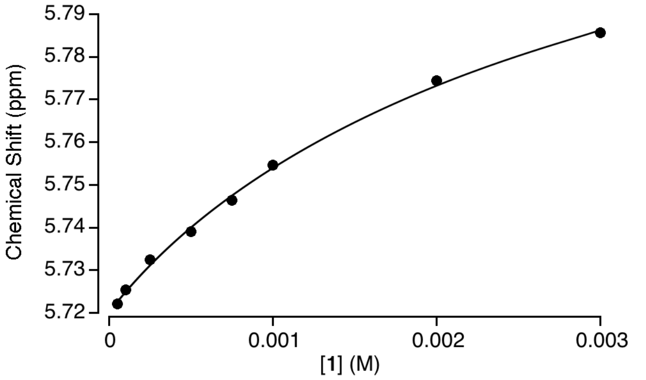

Figure 4 Plot of chemical shift of H_b versus [**1**] used to determine the self-association constant K_s = 480 ± 81 M^{-1} for **1**.

X-ray Crystal Structure of 1. We were fortunate to obtain single crystals of **1** by recrystallization from mixtures of EtOH and H_2O and to solve its structure by x-ray crystallography (CCDC-1949769). Figure 5a and 5b show stereoscopic representations of the two independent molecules of **1** in the crystal. The molecule of **1** in Figure 5a is C_2-symmetric and features an out-of-plane helical distortion that renders it chiral. Similarly, the molecule of **1** in Figure 5b is skewed out-of-plane and is therefore chiral; it also includes a solvating CF_3CO_2H molecule. Interestingly, only one sense of handedness is present in the crystal structure of **1** and therefore the crystal is a conglomerate. Figure 5c shows a stereoview of how these two different molecules of 1 pack next to each other in the crystal. The external face of the triptycene unit of one molecule of **1** embraces the convex face of the glycoluril region of the adjacent molecule of **1** and vice versa. The fact that two different conformations were observed in the crystal and the ^{1}H NMR evidence of a π-stacked conformation presented above highlights the conformational flexibility of the acyclic CB[n] that enables it to bind to a wide variety of guests.[20]

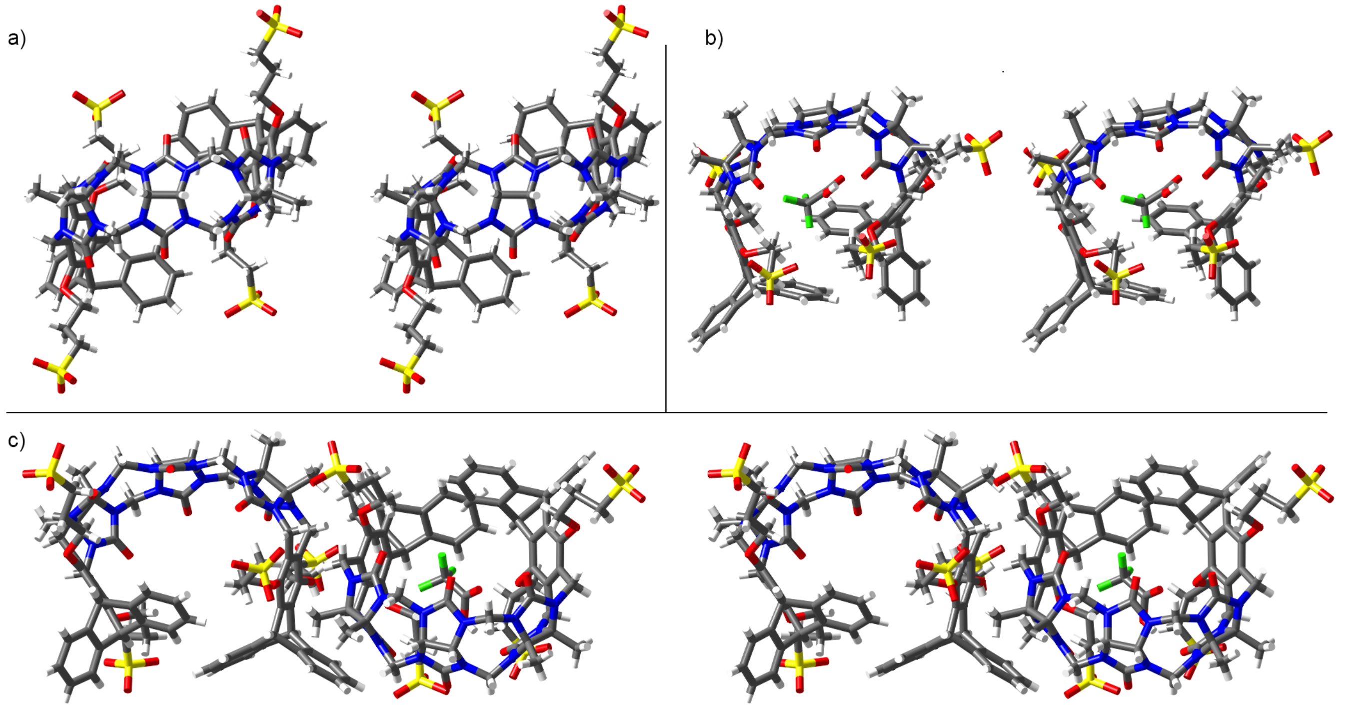

Figure 5 Cross-eyed stereoviews of the crystal structure of **1**. a&b) Two independent molecules of **1**. c) Packing of the two independent molecules of **1** into a dimeric unit. Color code: C, grey; H, white; N, blue; O, red; S, yellow; F, green.

Qualitative ^{1}H NMR Host•Guest Recognition Study. Next, we decided to perform a qualitative investigation of host•guest binding of **1** toward guests **4** – **19** (Figure 6) by ^{1}H NMR spectroscopy (Supporting Information). For example, Figure 3a-c shows the ^{1}H NMR spectra recorded for uncomplexed **8**, and 1:1 and 1:2 mixtures of **1** with **8**. As expected, the resonances for guest protons H_r, H_s, and H_t undergo substantial upfield shifts (> 1.5 ppm) upon formation of the **1•8** complex reflecting the encapsulation of the hydrophobic octylene chain inside the hydrophobic cavity of the host defined by the four aromatic rings of the triptycene sidewalls. The resonance for H_q also shifts significantly upfield (0.95 ppm) probably due to a helical twisting of **1** in the complex which deepens the cavity and brings H_q into proximity of a triptycene sidewall. The presence of separate resonances for free guest **8** and bound guest **8** (Figure 3b) at a 1:2 **1**:**8** stoichiometry reflects the slow kinetics of host•guest exchange on the chemical shift timescale. Host **1** also undergoes significant changes in chemical shift upon formation of the **1•8** complex. For example, the triptycene bridgehead methine resonance (H_e) moves downfield by 0.3 ppm. Most significantly, however, the resonance for H_b undergoes a substantial downfield shift (≈ 1.78 ppm) upon complexation which indicates that guest binding unfolds the self-folded conformation described above. Similar qualitative binding studies were performed for the remainder of the guests. In accord with expectations, we find that the resonances for the hydrophobic regions of guests **4-19** undergo substantial upfield shifts upon complexation due to the shielding effect of the triptycene sidewalls. The complexes of **1** with guests **5** – **10**, **12**, **13**, **16**, **17**, and **18** display slow to intermediate exchange kinetics (e.g. two sets of broadened resonances) on the NMR timescale whereas guests **4**, **11**, **14** – **15**, and **19** – **26** display intermediate to fast (e.g. one set of broadened resonances) kinetics of exchange.

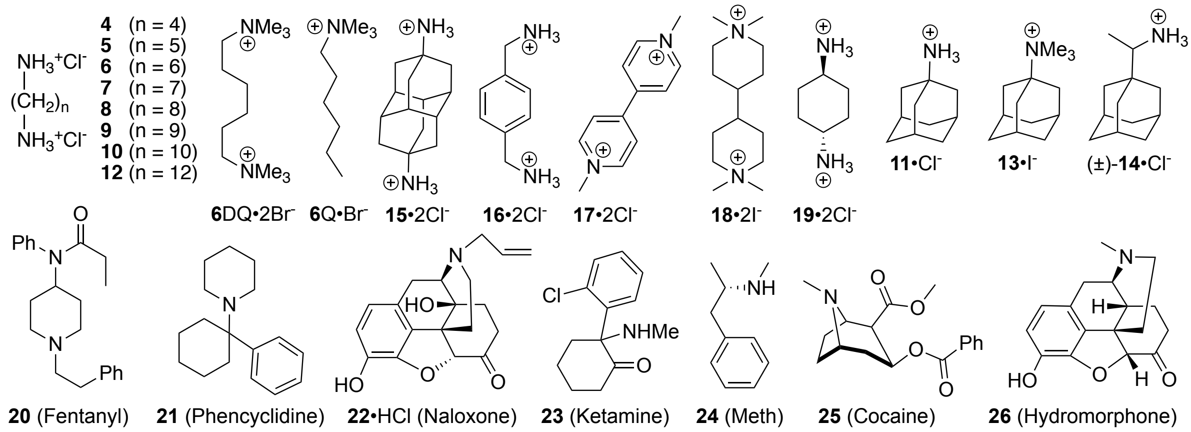

Figure 6 Structures of guests **4** – **26** used in this study.

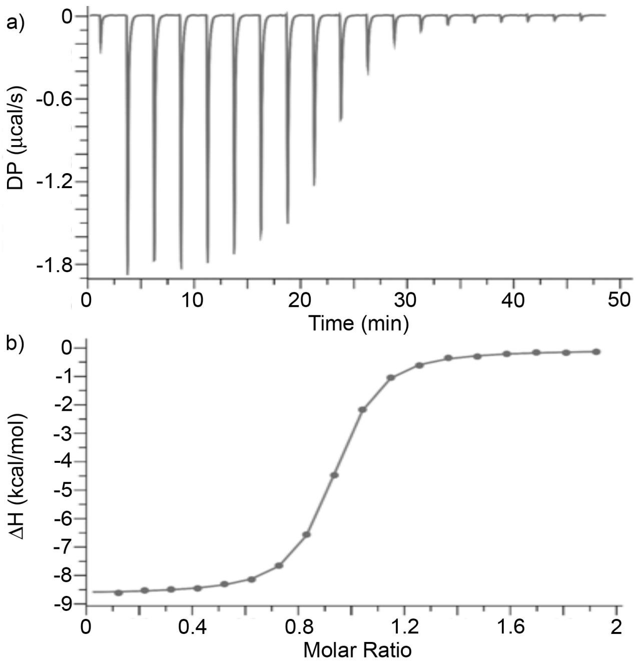

Figure 7 a) ITC thermogram recorded during the titration of host **1** (100 μM) in the cell with guest **5** (1.0 mM) in the syringe, b) Fitting of the data to a 1:1 binding model with K_a = 1.33 × 10^6 M^{-1}.

Measurement and Discussion of the Thermodynamic Parameters of Complex Formation. After qualitatively assessing the host•guest binding properties of **1** we decided to quantify the binding constants (K_a, M^{-1}). Given that CB[n]•guest binding constants typically exceed the dynamic range of ^{1}H NMR we decided to use ITC to simultaneously measure K_a and ΔH; ITC experiments were conducted in duplicate. For example, Figure 7a shows the thermogram recorded when a solution of **1** (100 μM) in the ITC cell was titrated with a solution of pentane diammonium **5** (1 mM) in the syringe. Figure 7b shows the fitting of the integrated heat values to a 1:1 binding model with K_a = 1.33 x 10^6 M^{-1} and ΔH = -8.58 kcal mol^{-1}. For the **1**•guest values with $K_a \leq 4.08 \times 10^6$ M^{-1} reported in Table 1 we performed similar direct ITC titrations. For complexes with higher K_a values, and therefore c-values that exceed the recommended range,[21] we turned to competitive ITC titrations. In competition ITC, a solution of the host and an excess of a weaker binding guest is titrated with a solution of the tighter binding guest. Using the known concentrations of host, weak guest, and host•weak guest K_a and ΔH as inputs allowed us to fit the thermogram to a competitive binding model in the PEAQ-ITC data analysis software to extract the thermodynamic constants for the tighter host•guest complexes reported in Table 1 (Supporting Information).

Table 1 Binding constants (K_a, M^{-1}) and binding enthalpies (ΔH, kcal mol^{-1}) measured for **1**•guest. Binding constants (K_a, M^{-1}) measured for **DimerTrip**•guest, and **M1**•guest complexes (298 K, 20 mM NaH_2PO_4 buffered water, pH 7.4).

G	**1**	**DimerTrip / M1** [f]
4	(2.92 ± 0.257) × 10^4 [a]	**DT:** (4.47 ± 0.75) × 10^3
	-6.03 ± 0.260	–
5	(1.33 ± 0.0308) × 10^6 [a]	**DT:** (1.23 ± 0.05) × 10^5
	-8.58 ± 0.021	–
6	(2.29 ± 0.166) × 10^7 [c]	**DT:** (8.81 ± 0.59) × 10^5
	-10.8 ± 0.044	**M1:** (5.05 ± 0.31) × 10^7
6DQ	(5.00 ± 0.209) × 10^7 [c]	**DT:** (1.26 ± 0.09) × 10^6
	-12.7 ± 0.028	**M1:** (8.93 ± 0.33) × 10^7
6Q	(1.20 ± 0.0329) × 10^6 [a]	**DT:** (3.41 ± 0.5) × 10^4
	-8.54 ± 0.027	**M1:** (1.24 ± 0.06) × 10^6
7	(7.24 ± 0.702) × 10^7 [c]	**DT:** (7.11 ± 0.32) × 10^5
	-10.1 ± 0.036	–
8	(1.41 ± 0.195) × 10^8 [d]	**DT:** (6.27 ± 0.41) × 10^5
	-11.5 ± 0.094	–
9	(2.42 ± 0.334) × 10^8 [d]	**DT:** (5.23 ± 0.34) × 10^5
	-11.4 ± 0.062	–
10	(2.81 ± 0.507) × 10^8 [e]	**DT:** (3.7 ± 0.16) × 10^5
	-11.3 ± 0.068	–
12	(4.55 ± 0.943) × 10^8 [d]	–

	-10.4 ± 0.064	–
11	(3.57 ± 0.139) × 10^5 [a]	–
	-4.83 ± 0.036	**M1:** (1.73 ± 0.20) × 10^7
13	(1.13 ± 0.109) × 10^7 [a]	**DT:** (1.04 ± 0.16) × 10^4
	-10.1 ± 0.119	**M1:** (1.70 ± 0.05) × 10^7
14	(4.08 ± 0.341) × 10^6 [a]	–
	-7.41 ± 0.084	–
15	(1.11 ± 0.0743) × 10^6 [a]	–
	-5.88 ± 0.049	–
16	(8.77 ± 0.493) × 10^6 [c]	**DT:** (7.1 ± 0.23) × 10^4
	-10.5 ± 0.044	**M1:** (1.67 ± 0.08) × 10^8
17	(5.81 ± 0.443) × 10^7 [c]	–
	-12.4 ± 0.045	**M1:** (4.69 ± 0.22) × 10^8
18	(3.57 ± 0.185) × 10^8 [d]	–
	-13.7 ± 0.039	–
19	(5.95 ± 0.222) × 10^4 [a]	**DT:** (3.29 ± 0.71) × 10^3
	-6.61 ± 0.088	**M1:** (1.95 ± 0.09) × 10^6
20	(1.33 ± 0.0414) × 10^7 [c]	–
	-14.7 ± 0.036	**M1:** (1.1± 0.04) × 10^7
21	(9.80 ± 0.317) × 10^4 [a]	–
	-5.09 ± 0.042	**M1:** (4.7 ± 0.5) × 10^4
22	(5.61 ± 0.583) × 10^4 [b]	–
	-3.98 ± 0.0942	–
23	(8.47 ± 3.10) × 10^3 [a]	–
	-4.95 ± 2.30	**M1:** (1.1 ± 0.1) × 10^4
24	(9.43 ± 0.198) × 10^5 [a]	–
	-9.63 ± 0.025	**M1:** (7.5 ± 2.9) × 10^6
25	(3.70 ± 0.111) × 10^4 [a]	–
	-9.99 ± 0.129	**M1:** (6.6 ± 0.4) × 10^5
26	(4.67 ± 0.446) × 10^3 [b]	–
	-8.92 ± 0.445	**M1:** 1.8 × 10^5

[a] Measured by direct ITC titration of host (100 μM) in the cell with guest (1 mM) in the syringe. [b] Measured by direct ITC titration of host (200 μM) in the cell with guest (>1 mM) in the syringe. [c] Measured by ITC competition assay using **19** (0.5 mM) as competitor included in the cell. [d] Measured by ITC competition assay using **5** (0.5 mM) as competitor included in the cell. [e] Measured by ITC competition assay using **5** (0.2 mM) as competitor included in the cell. [f] Data drawn from literature references.[14b, 16a, 22]

Magnitude of Binding Constants and Enthalpies. A perusal of Table 1 reveals that the K_a values for **1** with guests **4** – **19** fall in the range of 4670 – 4.55 x 10^8 M^{-1}; this large dynamic range of K_a values is desirable given their use as the blinded dataset in the upcoming SAMPL7 challenge. The complexes are all driven by favorable enthalpic contributions with ΔH values ranging from -3.98 to -14.7 kcal mol^{-1}. The substantial enthalphic driving forces observed are not unexpected given that cavity bound waters that lack a full complement of H-bonds are known to provide an enthalpic driving force for the complexes of macrocyclic CB[n].[3]

Influence of Diammonium Ion Length. CB[6] is known to preferentially bind to diammonium ions whose length (e.g. H_3N^+•••NH_3^+) matches the C=O•••O=C distances of the host; CB[6]•**5** and CB[6]•**6** display maximal affinity.[2a] An examination of Table 1 reveals a very different trend in K_a with the K_a values for increasing steadily from **1•4** (2.92 × 10^4 M^{-1}) to **1•8** (1.41 × 10^8 M^{-1}) and then plateaus at ≈ 10^8 M^{-1} for longer diammonium ions **9**, **10**, and **12**. Host **1** can accommodate longer diamines because it can flex and expand its cavity and because the $(CH_2)_3SO_3^-$ arms deepen the cavity while providing for new ammonium•••sulfonate interactions. Similar observations have been made previously for a carboxylate analogue of **M1**.[23]

Drugs of Abuse. Recently, we have found that acyclic CB[n]-type receptors (e.g. **M1**) bind tightly to neuromuscular blocking agents and function as *in vivo* reversal agents.[14a, 11b, 11c] More recently, we found that acyclic CB[n] bind strongly to methamphetamine and fentanyl and modulate the hyperlocomotion induced by methamphetamine *in vivo* (rats).[14b] Accordingly, we decided to determine the binding affinities of **1** toward a panel of drugs of abuse (**20** – **26**) by ITC (Table 1). Most notable is the interaction between **1** and fentanyl with K_d = 75 nM which makes it suitable as a potential *in vivo* reversal agent. The interaction between **1** and **21** – **26** are substantially weaker (K_a < 10^6 M^{-1}). The data in Table 1 also allow a comparison between **1** and **M1**. As can be seen, **M1** is often a slightly stronger host than **1**, most notably toward methamphetamine. This trend is not unexpected given that acyclic CB[n] based on glycoluril tetramer have more fully formed ureidyl C=O portals and larger cavities.[18]

Influence of Guest Charge. Compounds **6**DQ and **6**Q differ in the number of quaternary ammonium ions while maintaining a common hexylene hydrophobic core. Table 1 shows that the complex between **1** and dicationic guest **6**DQ (K_a = 5.00 × 10^7 M^{-1}) is 42-fold stronger than 1•**6**Q (K_a = 1.20 × 10^6 M^{-1}). Similar, but more pronounced trends are seen for CB[n]•guest complexes where an additional ion-dipole interaction commonly increases K_a by 10^2-10^3 M^{-1}.[5b, 24]

Influence of the Cationic Headgroup. Compounds **6** and **6**DQ as well as **11** and **13** differ only in the presence of primary ammonium (NH_3^+) or quaternary ammonium (NMe_3^+) ion centers. Table 1 shows that **1** binds the quaternary guests (**6**DQ and **13**) more tightly by 2.2-fold and 31.7-fold. Related effects have been seen for macrocyclic CB[7] complexes where the magnitude of the effect is dependent on the nature of the hydrophobic moiety.[2b, 25, 2e]

Influence of Guest Hydrophobic Residue. Macrocyclic CB[n]•guest complexes are very sensitive to the size and shape of the guest because the cavity of these hosts cannot easily expand its size to alleviate steric interactions.[2a, 2b] For example, CB[7] binds **11** (K_a = 4.23 x 10^{12} M^{-1}) more that 10^8-fold stronger than 3,5-dimethyladamantaneamine (memantine, K_a = 25000 M^{-1}).[2b] Consider the following series of guests: **6**, **16**, **17**, **18**, and **15**. Across this series, there is a constant number of C-atoms (6) in between the two ammonium ions centers. However, the total number of C-atoms in the hydrophobic moiety of the guest (**6**: 6; **16**: 8, **17**: 10, **18**: 10, and **15**: 14) and the nature of hydrophobicity of the moiety (e.g. aromatic **16** and **17** versus aliphatic **6**, **18**, **15**). As the number of C-atoms of the guest is increased one would expect larger K_a values due to more favorable desolvation of the larger guests upon complexation.

Conversely, as the size and cross-sectional area of the hydrophobic guest moiety is increased beyond an optimum one might expect decreased K_a values due to energetically costly expansion of the host cavity. Within this series of guests we observe a maximum K_a value of $(3.57 \pm 0.185) \times 10^8$ M^{-1} for **1•18**. As expected, the bulky multicyclic guests **21**, **22**, and **26** are quite poor guests for **1** with K_a in the $10^4 – 10^5$ M^{-1} range.

Comparisons between Hosts. Table 1 also presents the binding constants of two related hosts (**M1** and **DimerTrip**) drawn from the literature.[14b, 16a, 22] **DimerTrip** is an analogue of **1** that only contains two glycoluril rings. Accordingly, the cavity of **DimerTrip** is CB[6] sized and therefore smaller than the cavity of **1**. A comparison of the binding constants given in Table 1 reveals that **1** is a superior host compared to **DimerTrip** by 6.5 to 1086-fold. The highest selectivities are seen for bulky guests (**13**: 1086-fold; **10**: 760-fold) which cannot be fully encapsulated inside **DimerTrip** without substantial energetic penalties for cavity expansion. **M1** differs from **1** by the number of glycolurils (4 versus 3) unit and by the different sidewalls (benzene versus triptycene). A comparison of the K_a values in Table 1 toward a given guest shows that **M1** and **1** are comparable hosts in many cases (e.g. **6**, **6**DQ, **6**Q, **13**, **20**). Interestingly, host **M1** binds significantly stronger than **1** toward **11** (49-fold), **16** (19-fold), **17** (8-fold), and **24** (8-fold). Guests **16**, **17**, and **24** all contain aromatic ring binding sites which suggests that the hydrophobic box defined by **M1** is more appropriate for simultaneous edge-to-face and offset π-stacking with guests.[12] We conclude that **1** is a surprisingly good host that is nearly on par with the prototypical acyclic CB[n]-type receptor **M1**.

Conclusions

In summary, we have reported the synthesis of host **1** which is based on a central glycoluril trimer capped with two triptycene sidewalls. Host **1** is water soluble (3 mM) and does not undergo strong self-association in water ($K_s = 480$). In solution, **1** displays upfield chemical shifts for H_b of the triptycene sidewall (Figure 3d) which indicates a self-folded conformation. In constrast, the x-ray crystal structure of **1** displays two more open conformations where the triptycene sidewalls undergo an out-of-plane helical distorsion. In combination the ^1H NMR and x-ray results highlight the high conformational flexibility of **1** which stands in constrast to macrocyclic CB[n]. The geometries and thermodynamics of complexation between **1** and guests **4** – **26** were elucidated by ^1H NMR induced chemical shifts and measured by ITC. A subset of these K_a values form the blinded dataset for the SAMPL7 challenge.[17] We find that host **1** with its central glycoluril trimer is a superior host compared to previously synthesized host **DimerTrip**. Host **1** even displays K_a values toward many guests that are very close to those measured for **M1** which is the prototypical acyclic CB[n]-type host. Finally, host **1** is a powerful receptor for fentanyl which suggests its potential application as an *in vivo* sequestration agent.

Experimental.

General Experimental. Starting materials were purchased from commercial suppliers and used without further purification or were prepared by literature procedures.[18, 16c] Melting points were measured on a Meltemp apparatus in open capillary tubes and are uncorrected. IR spectra were recorded on a JASCO FT/IR 4100 spectrometer and are reported in cm^{-1}. NMR spectra were measured on commercial instruments operating at 400 or 600 MHz for ^1H and 100 or 150 MHz for ^{13}C using D_2O or DMSO-d_6 as solvents. Chemical shifts (δ) are referenced relative to the residual resonances for HOD (4.80 ppm) and DMSO-d_6 (2.50 ppm for ^1H, 39.51 ppm for ^{13}C). Mass spectrometry was performed using a JEOL AccuTOF electrospray instrument (ESI). ITC data were collected on a Malvern Microcal PEAQ-ITC instrument.

Host 1. A mixture of **2** (620 mg, 1.01 mmol) and **3** (1.332 g, 2.32 mmol) was dissolved in TFA/Ac_2O (1:1 (v:v), 40 mL). The solution was stirred under N_2 at 90 ˚C for 3.5 h and then was cooled to room temperature. EtOH (300 mL) was added to the reaction and the heterogenous mixture was stirred for 1 h. The precipitate was obtained by centrifugation and dried under high vacuum to obtain the crude product. The crude product was washed with EtOH (3 x 100 mL) and acetone (3 x 100 mL). After drying overnight, the crude product (300 mg) was recrystallized from H_2O/EtOH (1:10). The solid was dissolved in a minimal amount of water and the pH was adjusted to 7 with 1 mM NaOH. A red precipitate was observed and collected by centrifuged. The precipitate was dried and dissolved in a minimal amount of water and the pH was adjusted to 1 with 1mM HCl. The solid was dried and recrystallized from H_2O/EtOH (1:2). A thin white precipitate was observed very quickly and was gently collected by decantation. The solid was then dried under high vacuum overnight to give host **1** as a white powder (77.5 mg, 4.4% yield). M.p. >300 ˚C. ^1H NMR (600 MHz, D_2O, RT): δ 7.59 (s, 4H), 7.12 (s, 4H), 6.83 (s, 4H) 5.73 (s, 4H), 5.67 (s, 4H), 5.45 (d, J = 15.6, 4H), 5.32 (s, 2H), 5.04 (s, 4H), 4.20 (d, J = 16.4, 4H), 4.14 (d, J = 15.6, 8H), 3.91 (s, 4H), 3.24 (m, 8H), 2.37 (m, 8H), 1.73 (s, 6H), 1.65 (s, 6H). ^1H NMR (600 MHz, DMSO-d_6, RT): δ 7.48 (m, 8H), 7.15 (m, 4H), 6.98 (m, 4H), 5.79 (s, 4H), 5.44 (d, J = 15.2, 6H), 5.03 (d, J = 16.3, 4H), 4.07 (m, 12H), 3.82 (d, J = 7.2, 4H), 2.89 (m, 8H), 2.22 (m, 8H), 1.71 (s, 6H), 1.58 (s, 6H). ^{13}C NMR (600 MHz, D_2O, 1,4-dioxane as internal reference, RT): δ 155.5, 146.9, 144.1, 142.8, 139.1, 125.3, 124.4, 123.5, 122.9, 77.9, 76.9, 73.9, 70.9, 66.1, 56.9, 48.2, 47.5, 47.4, 35.3, 24.6, 16.2, 14.6. IR (ATR, cm^{-1}): 3574m, 2918w, 1614s, 1427s, 1027m, 877s, and 701s. HR-MS (ESI-MS negative) *m/z* 829.20204 ($[M + 1H - 3Na]^{2-}$), calculated 829.19495.

Acknowledgements. We thank the National Science Foundation (CHE-1404911 and CHE-1807486) and the National Institutes of Health (GM-132345 and GM-124270) for financial support.

Conflicts of interest

L.I. is an inventor on patents held by the University of Maryland on the use of acyclic CB[n]-type receptors in biomedical applications.

Notes and references

1) a) E. Masson, X. Ling, R. Joseph, L. Kyeremeh-Mensah and X. Lu, *RSC Adv.*, 2012, **2**, 1213-1247; b) S. J. Barrow, S. Kasera, M. J. Rowland, J. del Barrio and O. A. Scherman, *Chem. Rev.*, 2015, **115**, 12320-12406; c) D. Shetty, J. K. Khedkar, K. M. Park and K. Kim, *Chem. Soc. Rev.*, 2015, **44**, 8747-8761; d) S. Ganapati and L. Isaacs, *Isr. J. Chem.*, 2018, **58**, 250-263.

2) a) W. L. Mock and N.-Y. Shih, *J. Org. Chem.*, 1986, **51**, 4440-4446; b) S. Liu, C. Ruspic, P. Mukhopadhyay, S. Chakrabarti, P. Y. Zavalij and L. Isaacs, *J. Am. Chem. Soc.*, 2005, **127**, 15959-15967; c) M. V. Rekharsky, T. Mori, C. Yang, Y. H. Ko, N. Selvapalam, H. Kim, D. Sobransingh, A. E. Kaifer, S. Liu, L. Isaacs, W. Chen, S. Moghaddam, M. K. Gilson, K. Kim and Y. Inoue, *Proc. Natl. Acad. Sci. U. S. A.*, 2007, **104**, 20737-20742; d) S. Moghaddam, C. Yang, M. Rekharsky, Y. H. Ko, K. Kim, Y. Inoue and M. K. Gilson, *J. Am. Chem. Soc.*, 2011, **133**, 3570-3581; e) L. Cao, M. Sekutor, P. Y. Zavalij, K. Mlinaric-Majerski, R. Glaser and L. Isaacs, *Angew. Chem. Int. Ed.*, 2014, **53**, 988-993.

3) a) F. Biedermann, V. D. Uzunova, O. A. Scherman, W. M. Nau and A. De Simone, *J. Am. Chem. Soc.*, 2012, **134**, 15318-15323; b) F. Biedermann, W. M. Nau and H.-J. Schneider, *Angew. Chem. Int. Ed.*, 2014, **53**, 11158-11171; c) K. I. Assaf and W. M. Nau, *Chem. Soc. Rev.*, 2015, **44**, 394-418.

4) a) H. S. Muddana, C. Daniel Varnado, C. W. Bielawski, A. R. Urbach, L. Isaacs, M. T. Geballe and M. K. Gilson, *J. Comput.-Aided Mol. Des.*, 2012, **26**, 475-487; b) K. I. Assaf, M. Florea, J. Antony, N. M. Henrikson, J. Yin, A. Hansen, Z.-W. Qu, R. Sure, D. Klapstein, M. K. Gilson, S. Grimme and W. M. Nau, *J. Phys. Chem. B*, 2017, **121**, 11144-11162; c) A. Rizzi, S. Murkli, J. N. McNeill, W. Yao, M. Sullivan, M. K. Gilson, M. W. Chiu, L. Isaacs, B. C. Gibb, D. L. Mobley and J. D. Chodera, *J. Comput.-Aided Mol. Des.*, 2018, **32**, 937-963.

5) a) Y. H. Ko, E. Kim, I. Hwang and K. Kim, *Chem. Commun.*, 2007, 1305-1315; b) N. Saleh, A. L. Koner and W. M. Nau, *Angew. Chem. Int. Ed.*, 2008, **47**, 5398-5401; c) J. Del Barrio, P. Horton, D. Lairez, G. Lloyd, C. Toprakcioglu and O. Scherman, *J. Am. Chem. Soc.*, 2013, **135**, 11760-11763; d) L. Isaacs, *Acc. Chem. Res.*, 2014, **47**, 2052-2062.

6) G. Ghale and W. M. Nau, *Acc. Chem. Res.*, 2014, **47**, 2150-2159.

7) a) H. Yin and R. Wang, *Isr. J. Chem.*, 2017, **58**, 188-198; b) X. Zhang, X. Xu, S. Li, L. Li, J. Zhang and R. Wang, *Theranostics*, 2019, **9**, 633-645.

8) J. Tian, Z.-Y. Xu, D.-W. Zhang, H. Wang, S.-H. Xie, D.-W. Xu, Y.-H. Ren, H. Wang, Y. Liu and Z.-T. Li, *Nat. Commun.*, 2016, **7**, 11580.

9) a) Y. Ahn, Y. Jang, N. Selvapalam, G. Yun and K. Kim, *Angew. Chem. Int. Ed.*, 2013, **52**, 3140-3144; b) K. M. Park, J. Murray and K. Kim, *Acc. Chem. Res.*, 2017, **50**, 644-646; c) S. K. Samanta, J. Quigley, B. Vinciguerra, V. Briken and L. Isaacs, *J. Am. Chem. Soc.*, 2017, **139**, 9066-9074; d) C. Sun, H. Zhang, S. Li, X. Zhang, Q. Cheng, Y. Ding, L.-H. Wang and R. Wang, *ACS Appl. Mater. Interfaces*, 2018, **10**, 25090-25098; e) S. Zhang, Z. Dominguez, K. I. Assaf, M. Nilam, T. Thiele, U. Pischel, U. Schedler, W. M. Nau and A. Hennig, *Chem. Sci.*, 2018, **9**, 8575-8581; f) L. Zou, A. S. Braegelman and M. J. Webber, *ACS Cent. Sci.*, 2019, **5**, 1035-1043.

10) a) M. Stancl, M. Hodan and V. Sindelar, *Org. Lett.*, 2009, **11**, 4184-4187; b) M. Stancl, L. Gilberg, L. Ustrnul, M. Necas and V. Sindelar, *Supramol. Chem.*, 2014, **26**, 168-172; c) D. Bauer, B. Andrae, P. Gass, D. Trenz, S. Becker and S. Kubik, *Org. Chem. Front.*, 2019, DOI: 10.1039/c9qo00156e, Ahead of Print; d) W. Mao, D. Mao, F. Yang and D. Ma, *Chem. - Eur. J.*, 2019, **25**, 2272-2280.

11) a) D. Ma, G. Hettiarachchi, D. Nguyen, B. Zhang, J. B. Wittenberg, P. Y. Zavalij, V. Briken and L. Isaacs, *Nat. Chem.*, 2012, **4**, 503-510; b) U. Hoffmann, M. Grosse-Sundrup, K. Eikermann-Haerter, S. Zaremba, C. Ayata, B. Zhang, D. Ma, L. Isaacs and M. Eikermann, *Anesthesiology*, 2013, **119**, 317-325; c) F. Haerter, J. C. P. Simons, U. Foerster, I. Moreno Duarte, D. Diaz-Gil, S. Ganapati, K. Eikermann-Haerter, C. Ayata, B. Zhang, M. Blobner, L. Isaacs and M. Eikermann, *Anesthesiology*, 2015, **123**, 1337-1349; d) D. Diaz-Gil, F. Haerter, S. Falcinelli, S. Ganapati, G. K. Hettiarachchi, J. C. P. Simons, B. Zhang, S. D. Grabitz, I. M. Duarte, J. F. Cotten, K. Eikermann-Haerter, H. Deng, N. L. Chamberlin, L. Isaacs, V. Briken and M. Eikermann, *Anesthesiology*, 2016, **125**, 333-345; e) G. Hettiarachchi, S. K. Samanta, S. Falcinelli, B. Zhang, D. Moncelet, L. Isaacs and V. Briken, *Mol. Pharmaceutics*, 2016, **13**, 809-818; f) D. Sigwalt, D. Moncelet, S. Falcinelli, V. Mandadapu, P. Y. Zavalij, A. Day, V. Briken and L. Isaacs, *ChemMedChem*, 2016, **11**, 980-989.

12) B. Zhang and L. Isaacs, *J. Med. Chem.*, 2014, **57**, 9554-9563.

13) D. Mao, Y. Liang, Y. Liu, X. Zhou, J. Ma, B. Jiang, J. Liu and D. Ma, *Angew. Chem. Int. Ed.*, 2017, **41**, 12614-12618.

14) a) D. Ma, B. Zhang, U. Hoffmann, M. G. Sundrup, M. Eikermann and L. Isaacs, *Angew. Chem. Int. Ed.*, 2012, **51**, 11358-11362; b) S. Ganapati, S. D. Grabitz, S. Murkli, F. Scheffenbichler, M. I. Rudolph, P. Y. Zavalij, M. Eikermann and L. Isaacs, *ChemBioChem*, 2017, **18**, 1583-1588.

15) E. G. Shcherbakova, B. Zhang, S. Gozem, T. Minami, Y. Zavalij Peter, M. Pushina, L. Isaacs and P. J. Anzenbacher, *J. Am. Chem. Soc.*, 2017, **139**, 14954-14960.

16) a) W. Liu, X. Lu, Z. Meng and L. Isaacs, *Org. Biomol. Chem.*, 2018, **16**, 6499-6506; b) W. Liu, X. Lu, W. Xue, S. K. Samanta, P. Y. Zavalij, Z. Meng and L. Isaacs, *Chem. - Eur. J.*, 2018, **24**, 14101-14110; c) X. Lu, S. K. Samanta, P. Y. Zavalij and L. Isaacs, *Angew. Chem., Int. Ed.*, 2018, **57**, 8073-8078.

17) L. Isaacs, The SAMPL7 Blind Prediction Challenges for Computational Chemistry, https://github.com/MobleyLab/SAMPL7, Accessed September 27, 2019.

18) L. Gilberg, B. Zhang, P. Y. Zavalij, V. Sindelar and L. Isaacs, *Org. Biomol. Chem.*, 2015, **13**, 4041-4050.

19) F. Diederich, *Angew. Chem., Intl. Ed. Engl.*, 1988, **27**, 362-386.

20) B. Zhang, P. Y. Zavalij and L. Isaacs, *Org. Biomol. Chem.*, 2014, **12**, 2413-2422.

21) a) T. Wiseman, S. Williston, J. F. Brandts and L.-N. Lin, *Anal. Biochem.*, 1989, **179**, 131-137; b) J. Broecker, C. Vargas and S. Keller, *Anal. Biochem.*, 2011, **418**, 307-309.

22) W. Xue, P. Y. Zavalij and L. Isaacs, *Org. Biomol. Chem.*, 2019, **17**, 5561-5569.

23) D. Ma, P. Y. Zavalij and L. Isaacs, *J. Org. Chem.*, 2010, **75**, 4786-4795.

24) a) M. Shaikh, J. Mohanty, P. Singh, W. Nau and H. Pal, *Photochem. Photobiol. Sci.*, 2008, **7**, 408-414; b) I. Ghosh and W. M. Nau, *Adv. Drug Delivery Rev.*, 2012, **64**, 764-783.

25) E. Masson, Y. M. Shaker, J.-P. Masson, M. E. Kordesch and C. Yuwono, *Org. Lett.*, 2011, **13**, 3872-3875.

Graphical Abstract

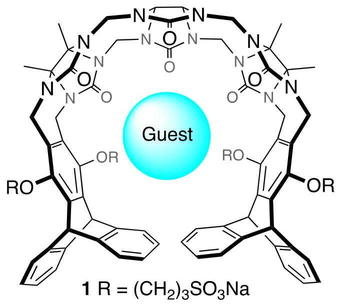

1 R = $(CH_2)_3SO_3Na$

The synthesis, characterization, and molecular recognition properties of **1** toward organic ammonium ions in water is reported.